

## Films of Lutetium Bisphthalocyanine Nanowires As Electrochemical Sensors

Mónica Gay Martín,<sup>†</sup> Maria Luz Rodríguez-Méndez,<sup>\*†</sup> and Jose Antonio de Saja<sup>‡</sup><sup>†</sup>Inorganic Chemistry Department, ETS Ingenieros Industriales and <sup>‡</sup>Condensed Matter Physics Department, Faculty of Science, University of Valladolid, 47011 Valladolid, Spain

Received June 26, 2010. Revised Manuscript Received November 3, 2010

Lutetium bisphthalocyanine (LuPc<sub>2</sub>) nanowires have been successfully obtained by electrophoretic deposition (EPD). The influence of the deposition conditions and annealing in the structure of the films has been studied by AFM, SEM, X-ray diffraction (XRD), UV–vis absorption, and near-infrared (NIR). The electrochemical properties of the EDP films immersed in different electrolytic solutions (KCl, MgCl<sub>2</sub>, KClO<sub>4</sub>, HCl, and NaOH) indicate that anions diffuse inside the film to maintain the electroneutrality and the kinetics follows the Randles-Sevcik equation. The stability of the response increases strongly upon annealing due to the improvement of the adhesion of the sensitive material to the substrate. The EPD films have been successfully used to detect caffeic acid (an antioxidant of interest in the food industry). The anodic peak associated with the oxidation of caffeic acid appears at 0.54 V and is linearly dependent on the caffeic acid concentration in the  $6 \times 10^{-5}$  M to  $5 \times 10^{-4}$  M range with a detection limit of  $3.12 \times 10^{-5}$  M. The electrochemical behavior of the annealed LuPc<sub>2</sub> EPD films is similar to that observed using Langmuir–Blodgett (LB) nanostructured films. However, the different molecular organization of the molecules inside the film causes differences in the shape and position of the peaks. Although LuPc<sub>2</sub> sensors prepared with both EPD and LB techniques provide stable and reproducible responses, the use of EPD is preferred for real sensing applications because of its lower cost, shorter preparation time, and longer lifetime.

## 1. Introduction

Phthalocyanine compounds are among the most interesting materials for sensing applications because their optical, electronic, and electrochemical properties can be modified under different conditions.<sup>1–3</sup> The electrochemical behavior of electrodes chemically modified with phthalocyanines has been exploited to construct potentiometric or amperometric sensors for the analysis of a variety of liquids.<sup>4–6</sup> The control of the structure at the nanometric level (size, orientation, alignment, thickness, etc.) is an important tool used to modulate the sensor response. Nanostructured thin films have shown great potential in improving the sensitivity and reliability of chemical sensors.<sup>7,8</sup>

Typical methods used to fabricate nanostructured phthalocyanine films include drop-cast,<sup>9</sup> self-assembly monolayer,<sup>10</sup>

self-assembly multilayer (or layer-by-layer),<sup>11–13</sup> the Langmuir–Blodgett technique,<sup>14–17</sup> and the thermal vacuum evaporation technique.<sup>18</sup> Compared with these methods, which are accomplished at high cost and long experimental time, electrophoretic deposition (EPD) can be an alternative way to prepare thin films with low cost, simple apparatus, little restriction of the shape of substrate and with a short formation time. EPD has recently been used to deposit unique nanostructured films consisting of nanowires of metallophthalocyanines such as copper phthalocyanine (CuPc)<sup>19–22</sup> or aluminum phthalocyanine (AlPc).<sup>23</sup> Studies of their morphology and their optical properties have been done. Attempts have also been made to prepare nanowires of gadolinium and europium double-decker phthalocyanines.<sup>24–26</sup>

Lanthanide bisphthalocyanines (LnPc<sub>2</sub>) are of special interest as sensitive materials due to their rich electrochemistry, which is

\*Corresponding author. Phone: +34 983423540. E-mail: mluz@eis.uva.es.

(1) Kadish, K. M.; Smith, K. M.; Guillard, R. *The Porphyrin Handbook*; Academic Press: San Diego, 2000; Vols. 1–10.

(2) Giancane, G.; Guascito, M. R.; Malitesta, C.; Mazzotta, E.; Picca, R. A.; Valli, L. *J. Porphyrins Phthalocyanines* **2009**, *13*, 1129–1139.

(3) Jiang, J.; Kasuga, K.; Arnold, D. P. In *Supramolecular Photoactive and electroactive materials*, Nalwa, H. S., Eds.; Academic Press: New York, 2001; p 113.

(4) Ou, Z. P.; Jiang, Z.; Chen, N. S.; Huang, J.; Shen, J.; Kadish, K. M. *J. Porphyrins Phthalocyanines* **2008**, *12*, 1123–1133.

(5) De Saja, J. A.; Rodríguez-Méndez, M. L. *Adv. Colloid Interface Sci.* **2005**, *116*, 1–11.

(6) Damos, F. S.; Luz, R. C. S.; Tanaka, A. A.; Kubota, L. T. *Anal. Chim. Acta* **2010**, *664*, 144–150.

(7) Rodríguez-Méndez, M. L. In *Encyclopedia of Sensors*, Grimes, C. S.; Dickey, E. C.; Pishko, M. V., Eds.; American Scientific Publishers: New York, 2006; Vol 9, p 111.

(8) Penza, M.; Rossi, R.; Alvisi, M.; Signore, M. A.; Serra, E.; Paolesse, R.; D'Amico, A.; Di Natale, C. *Sens. Actuators, B* **2010**, *144*, 387–394.

(9) Yang, Z.-Y.; Gan, L.-H.; Lei, S.-B.; Wan, L.-J.; Wang, C.; Jiang, J.-Z. *J. Phys. Chem. B* **2005**, *109*, 19859–19865.

(10) Matemadombo, F.; Durmus, M.; Togo, C.; Limson, J.; Nyokong, T. *Electrochim. Acta* **2009**, *54*, 5557–5565.

(11) Santos, A. C.; Zucolotto, V.; Constantino, C. J. L.; Cunha, H. N.; Dos Santos, J. R., Jr; Eiras, C. J. *Solid State Electrochem.* **2007**, *11*, 1505–1510.

(12) Alessio, P.; Rodríguez-Méndez, M. L.; De Saja Sáez, J. A.; Constantino, C. J. L. *Phys. Chem. Chem. Phys.* **2010**, *12*, 3972–3983.

(13) Zhao, W.; Tong, B.; Pan, Y.; Shen, J.; Zhi, J.; Shi, J.; Dong, Y. *Langmuir* **2009**, *25*, 11796–11801.

(14) Arrieta, A.; Rodríguez-Méndez, M. L.; De Saja, J. A. *Sens. Actuators, B* **2003**, *95*, 357–365.

(15) Rodríguez-Méndez, M. L.; De Saja, J. A. *J. Porphyrins Phthalocyanines* **2009**, *13*, 606–615.

(16) Gorbunova, Y.; Rodríguez-Méndez, M. L.; Kalashnikova, I. P.; Tomilova, L.; De Saja, J. A. *Langmuir* **2001**, *17*, 5004–5010.

(17) Liu, Y. L.; Wang, W. J.; Gao, X. X.; Li, S. H.; Li, Y. *Spectrosc. Spect. Anal.* **2008**, *28*, 2375–2379.

(18) Rodríguez-Méndez, M. L.; Aroca, R.; De Saja, J. A. *Spectrochim. Acta* **1993**, *49A*, 965–973.

(19) Yamanouchi, H.; Irie, K.; Saji, T. *Chem. Lett.* **2000**, *29*, 10–11.

(20) Takada, M.; Yoshioka, H.; Tada, H.; Matsushige, K. *Jpn. J. Appl. Phys.* **2002**, *41*, L73–L75.

(21) Xu, H.-B.; Chen, H.-Z.; Xu, W.-J.; Wang, M. *Chem. Phys. Lett.* **2005**, *412*, 294–298.

(22) Tong, W. Y.; Djuricic, A. B.; Ng, A. M. C.; Chan, W. K. *Thin Solid Films* **2007**, *515*, 5270–5274.

(23) Yang, Z.; Pu, H. *Mater. Chem. Phys.* **2005**, *94*, 202–206.

(24) Chen, H.-Z.; Cao, L.; Zhou, H.-B.; Rong, Y.; Wang, M. *J. Cryst. Growth* **2005**, *281*, 530–537.

(25) Bai, R.; Shi, M. M.; Ouyang, M.; Cheng, Y.; Zhou, H.; Yang, L.; Wang, M.; Chen, H. *Thin Solid Films* **2009**, *517*, 2099–2105.

(26) Bai, R.; Chen, H.-Z.; Zhou, H.-B.; Shi, M.-M.; Wang, M. *J. Cryst. Growth* **2005**, *285*, 183–190.

related to the accessibility of a range of oxidation states centered on the ligand.<sup>15,27–30</sup> Voltammetric sensors based on Langmuir–Blodgett (LB) films of a number of bisphthalocyanine derivatives have been prepared. The electrodes show distinct responses when immersed in different solutions, and this is the basis of their use as electrochemical sensors.<sup>14,31,32</sup> It has been demonstrated that nanostructured LuPc<sub>2</sub> LB films show faster kinetics and better reproducibility than non-nanostructured electrodes,<sup>14</sup> and these properties make them more suitable for sensing applications. However, the high cost and long time needed to prepare LB electrodes are major constraints for practical applications.

The objective of this work is to obtain and characterize nanowires of a lanthanide bisphthalocyanine containing lutetium as the central metal atom (LuPc<sub>2</sub>) using electrophoretic deposition (EPD) and to analyze the sensing properties of the obtained film. Therefore, films have been generated under different electrochemical conditions. After the structural characterization, the films have been employed as the working electrode in cyclic voltammetry experiments. The electrochemical responses toward different ionic solutions and the kinetics of the responses have been analyzed and compared with that observed in nanostructured LB films. Finally, the electrodes have been used to detect caffeic acid (an antioxidant of great interest in the food industry), and their sensing properties have been evaluated.

## 2. Materials and Methods

The LuPc<sub>2</sub> (with a sandwich structure) was synthesized as previously reported.<sup>27,33</sup> The lutetium bisphthalocyanine was submitted for elemental analysis and the results obtained for LuC<sub>64</sub>H<sub>32</sub>N<sub>16</sub> were C, 64.06%; H, 2.68%; N, 18.68%; and C, 64.07%; H, 2.70%; N, 18.70% for calculated and found, respectively. According to previous works,<sup>33</sup> the IR (KBr) spectra obtained for the LuPc<sub>2</sub> shows the main peaks at 724 cm<sup>-1</sup>, 1115 cm<sup>-1</sup>, 1320 cm<sup>-1</sup>, 1450 cm<sup>-1</sup>, and 1516 cm<sup>-1</sup>. The <sup>1</sup>H NMR of the lutetium bisphthalocyanine (dissolved in CDCl<sub>3</sub>) is included in the Supporting Information. The chemical shifts obtained were  $\delta = 9.20$  ppm (atom a, 1H),  $\delta = 7.95$  ppm (atom d, 1H),  $\delta = 7.89$  ppm (atom c, 1H), and  $\delta = 7.74$  ppm (atom b, 1H). All these experiments confirm the purity of the LuPc<sub>2</sub>. All reactants were purchased from Panreac and were used without further purification. Indium/tin oxide (ITO) coated glass slides (2.5 cm × 1 cm) were used as the cathode and a platinum plate was used as the anode in the EPD experiments. Before deposition, the ITO glass slides were sonicated for 5 min in acetone and finally cleaned with chloroform. The electrophoretic solution consisted of a lutetium bisphthalocyanine (10<sup>-4</sup> M) and trifluoroacetic acid (0.06M) mixture diluted in chloroform. The electrodes were kept at a constant distance (1 cm) and a direct current density of 20 V.cm<sup>-1</sup> was applied between the two electrodes. LuPc<sub>2</sub> films were prepared at three different deposition times: 40 s, 60 s, and 180 s. After deposition, films were annealed at 150 °C for 1 h (at atmospheric pressure) in order to improve their electrochemical stability.

The Langmuir–Blodgett (LB) films were prepared in a KSV 2000 LB trough equipped with a Wilhelmy plate to measure the surface pressure. Arachidic acid was used for reducing the rigidity of the Langmuir films. A mixture of bisphthalocyanine and arachidic acid (1:1) was dissolved in chloroform (10<sup>-4</sup> M) and spread onto ultrapure water, which was kept at a constant temperature (20 °C). The floating molecules were compressed at a speed of 5 mm.min<sup>-1</sup>, with a surface pressure of 40 mN·m<sup>-1</sup>; LB films were deposited onto ITO glass substrates, with a substrate speed of 3 mm.min<sup>-1</sup>. A Z deposition type was observed. Under these conditions, 20 ML films were obtained.

UV–vis absorption spectra were recorded using a Shimadzu UV-1603 spectrophotometer. NIR transmittance spectra were carried out in a Nicolet Magna-IR 760 spectrophotometer. AFM images were registered in tapping mode using a microscope from Digital Instruments (multimode MMAFM-2). SEM images were recorded in a Jeol JSM-S820. XRD data were obtained using a Philips PW1830 diffractometer. <sup>1</sup>H NMR spectrum was recorded with a Bruker Avance 400 Ultrashield instrument and was referred to TMS. Elemental analysis was performed with a Perkin-Elmer 2400B microanalyzer. Electrochemical measurements were carried out using a Parstat 2273 potentiostat (EG&G) using a conventional three electrode cell. The LuPc<sub>2</sub> nanowires deposited on the ITO were used as the working electrode, a platinum sheet was used as the counter electrode and a Ag/AgCl electrode was used as the reference electrode. Cyclic voltammograms were registered in 0.1 M aqueous solutions of KCl, MgCl<sub>2</sub>, KClO<sub>4</sub>, HCl, and NaOH from -1.0 to 1.3 V (except in the case of HCl, which was from -0.5 to 1.3 V), at a scan rate of 0.05 V.s<sup>-1</sup>. Caffeic acid (5 × 10<sup>-4</sup> M) was dissolved in a solution of 12% (v/v) ethanol and 0.033 M L-tartaric acid, pH 3.6. The voltammograms were recorded from -0.5 to 1.3 V (vs Ag/AgCl). For the detection limit studies, the caffeic acid concentrations used were 6 × 10<sup>-5</sup> M, 1 × 10<sup>-4</sup> M, 3 × 10<sup>-4</sup> M, and 5 × 10<sup>-4</sup> M.

## 3. Results and Discussion

### 3.1. Film Morphology of LuPc<sub>2</sub> Electrodeposited Films.

EPD films were prepared at deposition times of 40, 60, and 180 s. Initially, the UV–vis spectra of the prepared films showed a purple color (maximum at 520 nm) that corresponded to the protonated species.<sup>7,25–27</sup> After preparation, the films were washed with deionized water. Then, spectra were recorded every 2.5 min (Figure 1a). It could be observed that the neutral green species (with a maximum at 667 nm) was progressively formed. After 30 min, the formation of the green form was completed.

When the green neutral form was obtained, the spectra were similar to those recorded in chloroform solutions with an intense Q-band at 663, 666, and 667 nm for films prepared at 40, 60, and 180 s, respectively (Figure 1b). The similarity to the spectra registered in solution (Q-band at 659 nm) excluded the occurrence of polymerization processes. According to the exciton theory,<sup>35</sup> the observed bathochromic shift of the Q-band can be associated with the formation of J-aggregates. This result is in good agreement with the UV–vis spectra previously published of LuPc<sub>2</sub> LB films where the formation of J-aggregates has been demonstrated.<sup>36</sup> In such films, the molecules are arranged with their main axis perpendicular to the substrate.<sup>37,38</sup>

The films were then annealed (1 h, 150 °C, atmospheric pressure) to improve the electrochemical stability (see Electrochemical Results section). The thermal treatment caused a drastic

(27) Tomilova, L. G.; Chernykh, E. V.; Gavrilov, V. I.; Shelepin, I. V.; Derkacheva, V. M.; Luk'yanets, E. A. *Zh. Obshch. Khim.* **1982**, *52*, 2606.

(28) Bouvet, M.; Parra, V.; Locatelli, C.; Xiong, H. *J. Porphyrins Phthalocyanines* **2009**, *13*, 84–91.

(29) Acikbas, Y.; Eyyapan, M.; Ceyhan, T.; Çapan, R.; Bekaroglu, O. *Sens. Actuators, B* **2009**, *135*, 426–429.

(30) Selector, S. L.; Arslanov, V. V.; Gorbunova, Y. G.; Raitman, O. A.; Sheinina, L. S.; Birin, K. P. *J. Porphyrins Phthalocyanines* **2008**, *12*, 1154–1162.

(31) Apetrei, C.; Rodríguez-Méndez, M. L.; Parra, V.; Gutierrez, F.; De Saja, J. A. *Sens. Actuators, B* **2004**, *103*, 145–152.

(32) Casilli, S.; De Luca, M. A.; Apetrei, C.; Parra, V.; Arrieta, A.; Valli, L.; Jiang, J.; Rodríguez-Méndez, M. L.; De Saja, J. A. *Appl. Surf. Sci.* **2005**, *246*, 304–313.

(33) Linaje, M.; Quintanilla, M. C.; González, A.; Del Valle, J. L.; Alcaide, G.; Rodríguez-Méndez, M. L. *Analyst* **2000**, *125*, 341–346.

(34) Rodríguez-Méndez, M. L.; Aroca, R.; De Saja, J. A. *Spectrochim. Acta* **1993**, *49A*, 965–973.

(35) Mc Rae, E. G.; Kasha, M. In *Physical Processes in Radiation Biology*; Augenstein, L.; Manson, R.; Rosenberg, B., Eds.; Academic Press: New York, 1964.

(36) Rodríguez-Méndez, M. L.; Gorbunova, Y.; De Saja, J. A. *Langmuir* **2002**, *18*, 9560–9565.

(37) Moreira, W. C.; Aroca, R. *Spectrochim. Acta* **1995**, *51*, 2325–2334.

(38) Souto, J.; de Saja, J. A.; Aroca, R.; Rodríguez-Méndez, M. L. *Synth. Met.* **1993**, *54*, 229–235.

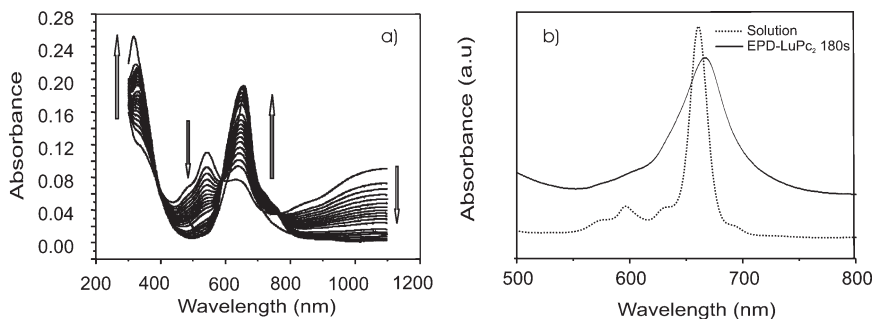


**Figure 1.** Electronic absorption spectra of (a) a fresh EPD film deposited at 180 s. Spectra were recorded every 2.5 min. (b) Electronic absorption spectra of a LuPc<sub>2</sub> chloroform solution 10<sup>-4</sup> M (dotted line) and of the EPD film in the neutral green form (solid line).

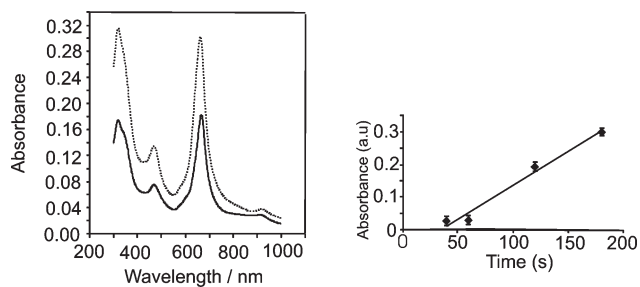


**Figure 2.** (a) Electronic absorption spectra of a LuPc<sub>2</sub> film deposited by EPD during 180 s, before (—) and after (---) annealing. (b) Linear relationship between the absorbance and the deposition time after annealing.

increase of the absorbance of the films. A small hypsochromic shift was also observed (in films deposited for 180 s, the Q-band shifted from 667 to 663 nm) (Figure 2a). The increase in the absorbance can be associated to the reorganization and coalescence of smaller nanowires giving rise to larger and thicker structures.

The absorbance of the Q-band and the Soret band (at 340 nm) increased linearly with the deposition time (Figure 2b). This effect is related to the number of LuPc<sub>2</sub> equivalents that migrate to the cathode and are electrodeposited onto the ITO surface. Considering that the absorbance of the Q-band of a 10 ML LB film of LuPc<sub>2</sub> is 0.1521, the calculated thickness of the EPD films (expressed as “number of monolayers”) was 1.52, 2.10, and 12.00 for EPD films deposited during 40, 60, and 180 s, respectively. In the case of annealed films, the number of “monolayers” obtained has been 2.32, 4.73, and 19.90 for 40, 60, and 180 s, respectively.

The NIR transmittance spectra of the electrodeposited films (see Supporting Information) showed a broad peak at 1424 nm with a shoulder at 1264 nm. These broad peaks are assigned to an intramolecular charge transfer between the two phthalocyanine rings of the  $Pc^{2-}LuPc^{\bullet-}$  molecule. The dianion *Pc* ring acts as an electron donor and the radical monoion *Pc* ring as an electron acceptor. Such bands have also been observed in LB films and confirm that the LuPc<sub>2</sub> molecules are in their neutral radical state.<sup>39</sup>

The morphology of the LuPc<sub>2</sub> thin films fabricated by EPD was analyzed by means of AFM and SEM. Figure 3a,b,c show the AFM topographic images of the LuPc<sub>2</sub> EPD films deposited onto ITO substrates at the three studied deposition times. As shown in Figure 3, the formation of LuPc<sub>2</sub> nanowires was achieved under the electrophoretic conditions used. These results are in good agreement with the previous studies using other phthalocyanine

compounds.<sup>24,26</sup> The mechanism of electrophoretic deposition involves two steps. In the first step, protonated LuPc<sub>2</sub> species formed by the action of the acidic media migrate toward the oppositely charged electrode. In the second step, the LuPc<sub>2</sub> particles nucleate and grow at the electrode surface. The rapid nucleation rate is responsible for the formation of the nanostructures.<sup>40</sup> As reported in Table 1, the thickness of the nanowires and the roughness of the films increased with the deposition time. Also, an increase of the number of V-type structures could be observed with increasing deposition time.

AFM images of annealed films (Figure 3d,e,f) clearly show that the thermal treatment causes the coalescence of smaller nanowires giving rise to larger and thicker structures. At the same time, an increase of the number of branched structures and of the rugosity is observed.<sup>25</sup> The increase of the thickness can explain the enhancement in the absorbance observed in the UV–vis spectra (Figure 2b). Similar results were obtained using SEM microscopy (see Supporting Information).

In order to establish the degree of order of the obtained structures, X-ray diffraction analysis were carried out (Figure 4). Before annealing, an intense peak appears at  $2\theta = 29.60$  for films obtained at 40 s, corresponding with a distance of 3.01 Å. According to the previously published structure of the LuPc<sub>2</sub> molecules,<sup>41</sup> this peak can be associated with a stacking of the LuPc<sub>2</sub> molecules with the aromatic rings perpendicular to the substrate other. This result agrees with the formation of J-aggregates observed in UV–vis spectra with the molecules with their main axis perpendicular to the substrate. An additional peak could be observed at  $2\theta = 6.97$  ( $d = 12.67$  Å), which implies the existence of a herringbone structure organization that could be located in the V-type structures (Figure 4). This peak is small in films deposited for 40 s and increases its relative intensity with the deposition time. After annealing, molecules can obtain enough energy to rearrange themselves and the peak at  $2\theta = 6.97$  increases its intensity (250 counts in films deposited at 180 s and 350 counts in annealed films).

In summary, nanowires are formed by stacking of the LuPc<sub>2</sub> molecules with the aromatic rings perpendicular to the substrate (as suggested by the observation of J-aggregates). AFM images show the existence of branched structures that could contain herringbone organization. When increasing the deposition times or when applying a thermal treatment, the size and thickness of the nanowires increase causing an enhancement of the absorbance. Simultaneously, the number of branched V-type structures

(40) Corni, I.; Ryan, M. P.; Boccacini, A. R. *J. Eur. Ceram. Soc.* **2008**, *28*, 1353–1367.

(41) Rousseau, R.; Aroca, R.; Rodríguez-Méndez, M. L. *J. Mol. Struct.* **1995**, *356*, 49–62.

(42) Toupanca, T.; Vincent, P.; Simon, J. *New J. Chem.* **1999**, *23*, 1001–1006.

(39) Markovitsi, D.; Tran-Thi, T. H.; Even, R.; Simon, J. *J. Chem. Phys. Lett.* **1987**, *137*, 107–112.

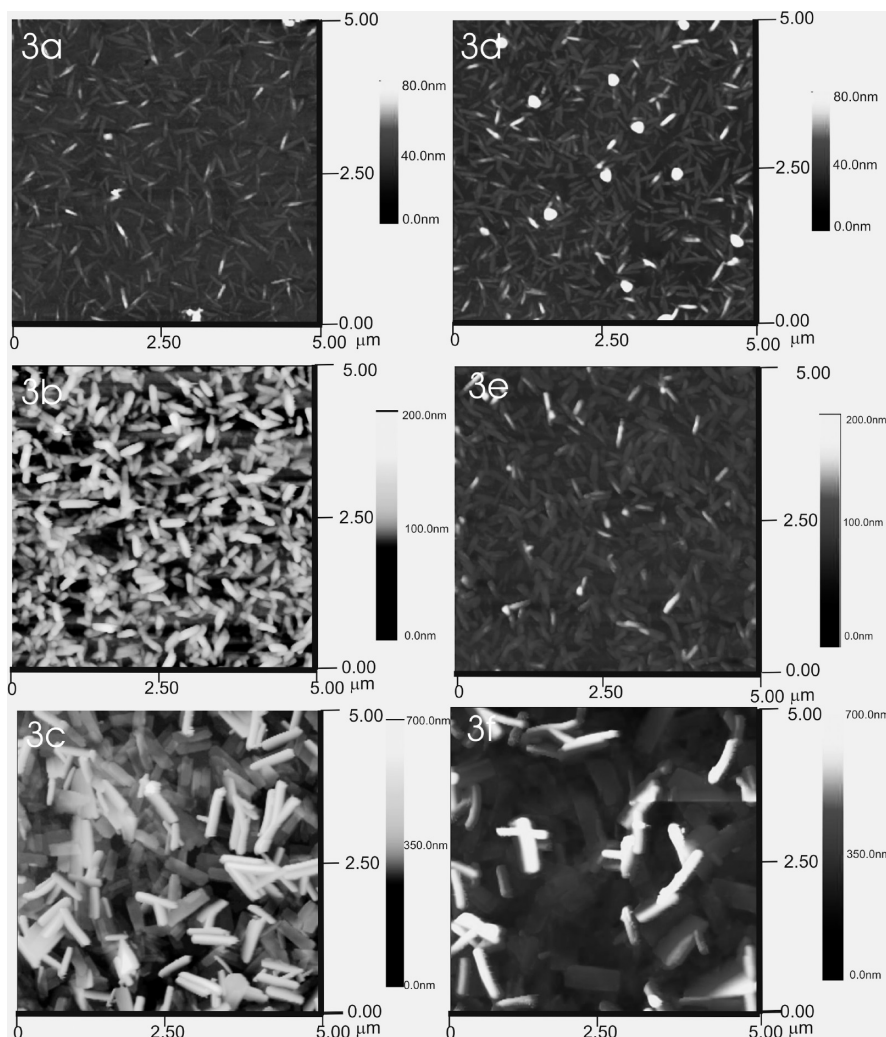


**Figure 3.** AFM images of LuPc<sub>2</sub> nanowires formed at 40, 60, and 180 s (a,b,c) before and (d,e,f) after annealing at 150 °C for 1 h.

**Table 1.** Size of the Nanowires and Structural Data of Films Obtained at Different Deposition Times<sup>a</sup>

deposition time (s)	40		60		180	
	a	b	a	b	a	b
diameter (nm)	30–60	80–100	95–100	90–130	100–120	200–400
length (nm)	200–400	250–300	300–450	350–500	600–800	900–1100
roughness (nm)	4.518	7.364	11.525	10.810	49.015	87.787
$R_{\max}$ (nm)	46.627	31.339	67.688	49.721	44.002	43.941
$R_z$ (nm)	20.937	20.289	51.568	33.473	27.336	31.679

<sup>a</sup>a, before annealing; b, after annealing.

increases (observed in the AFM images), enhancing the intensity of the X-ray peak at  $2\theta = 6.97$ .

**3.2. Electrochemical Response of the LuPc<sub>2</sub> Nanowires: Kinetics, Reproducibility, and Stability.** Electrochemical experiments were carried out by immersing the ITO electrodes in a variety of ionic solutions and registering the corresponding cyclic voltammograms. A clear voltammogram was obtained for the first cycle, but with successive cycles, the films became detached from the electrode and reproducible results could not be obtained. In contrast, highly reproducible voltammograms were obtained when using annealed films due to the improvement of the adhesion of the sensitive material to the substrate. The results described in the following paragraphs correspond to annealed films.

The electrochemical behavior of the LuPc<sub>2</sub> films electrodeposited for 40, 60, and 180 s is illustrated in Figure 5 using KCl as an

electrolyte. The voltammograms displayed two quasireversible processes corresponding to the one electron ring oxidation Lu(III)Pc<sub>2</sub>/Lu(III)Pc<sub>2</sub><sup>+</sup> (peak I): ( $E_{1/2} = 0.56$  V) and the one electron ring reduction Lu(III)Pc<sub>2</sub>/Lu(III)Pc<sub>2</sub><sup>-</sup> (peak II) ( $E_{1/2} = -0.42$  V) of the bisphthalocyanine molecule (In Figure 5,  $I_a$  means anodic wave and  $I_c$  means cathodic wave). As expected, the intensities of the peaks increase with the deposition time due to the increasing amount of phthalocyanine that migrates to the cathode.

This behavior is quite similar to the well-known electrochemical activity previously described for LB films<sup>14</sup> (Figure 6), with a few notable exceptions. Peak I appears at slightly higher potentials ( $E_{1/2} = 0.64$  V) in LB films due to the presence of the arachidic acid used to facilitate the deposition of the floating monolayers. In EPD films, a shoulder in the anodic wave of peak I (at ca. 0.5 V) was observed in thick films as a reflection of the coexistence of two

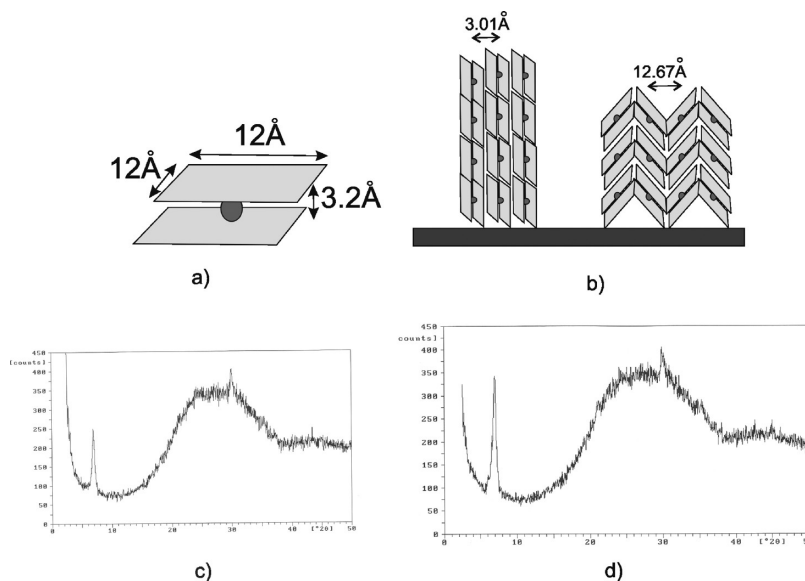


**Figure 4.** (a) Molecular structure of LuPc<sub>2</sub> and its dimensions. (b) Possible structure of the nanowires electrodeposited on the ITO substrate. (c) X-ray diffractogram of the film deposited at 180 s. (d) X-ray diffractogram of the annealed film deposited at 180 s.

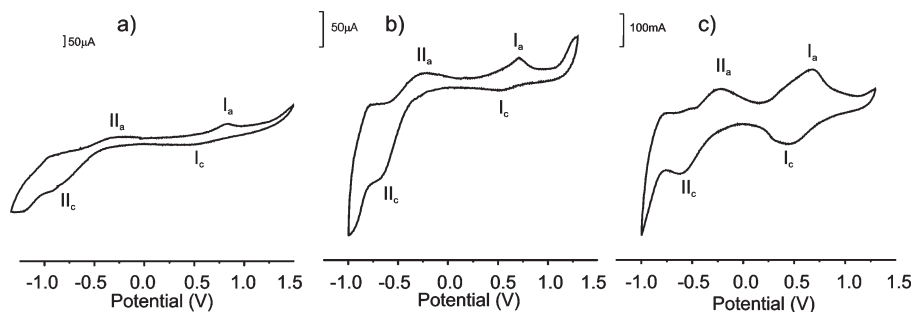


**Figure 5.** Cyclic voltammetry of LuPc<sub>2</sub> electrodeposited films at (a) 40 s, (b) 60 s, and (c) 180 s immersed in 0.1 M KCl.

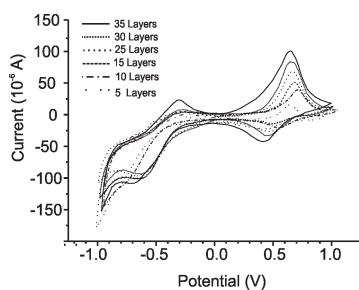


**Figure 6.** Electrochemical response of LB films of increasing thicknesses (5–35 monolayers) recorded at 0.050 V·s<sup>-1</sup> in a 0.1 M KCl solution.

structures within the film that has been observed in the XRD experiments. The existence of two classes of environments can give rise to the oxidation of Pc molecules at two different (although very close) electrochemical potentials. This shoulder increases in intensity when the deposition time is increased. For this reason, in films deposited at 40 s, only a certain asymmetry of the peak is noticed, whereas in films deposited for 180 s, the shoulder is clearly observed. In contrast, for the LB films, the intensity of peak I increased with the number of monolayers, but the shape of the curve did not change due to the homogeneity of films obtained by the deposition of successive monolayers.

Kinetic studies were carried out by recording the cyclic voltammograms of the EPD electrodes at different scan rates

(from 0.025 to 1.2 V·s<sup>-1</sup>). In all cases, the intensity of the redox peaks increased linearly with the square root of the scan rate (Figure 7) indicating the dominance of the diffusion controlled processes according to the Randles–Sevcik equation

$$I = 2.687 \times 10^5 n^{3/2} v^{1/2} D^{1/2} AC \quad (1)$$

where  $I$  is the peak current,  $A$  is the electrode surface area,  $D$  is the diffusion coefficient, and  $C$  is the bulk concentration. The diffusion coefficient ( $D$ ) can be calculated from the  $I$  versus  $v^{1/2}$  plot (Table 2). The Diffusion coefficients calculated are consistent with the results found in Langmuir–Blodgett films.<sup>14</sup>

In order to evaluate the stability of the EPD films, consecutive cycles were recorded in 0.1 M KCl solution. The nonannealed films were quite unstable and reproducible voltammograms could not be obtained. Nevertheless, the stability was significantly improved by using annealed films. The first scan of the thermally treated films was, expectedly, slightly different from the second cycle; subsequent scans were highly reproducible and the only noticeable change was a gradual decrease of the intensity of the peaks. The decrease of the intensity was more significant in the EPD films than in the LB films. In the EPD films, the intensity decreased by 50% after 75 scans, whereas in the LB films, the intensity decreased by 50% after 500 scans. When the cyclic voltammetry treatment was stopped, the EPD films were withdrawn from the solution and washed with milli-Q water to remove any adsorbed particle on the surface of the electrode. The films

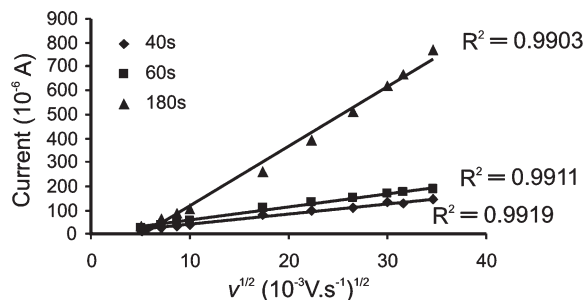


**Figure 7.** Plot of the intensity of the anodic wave of peak I vs the square root of the scan rate at the various annealing times (40, 60, and 180 s).

**Table 2. Diffusion Coefficient of the Films Deposited at Different Deposition Times**

deposition time (s)	diffusion coefficient ( $\text{cm}^2/\text{s}$ )
40	$2.11 \times 10^{-8}$
60	$3.46 \times 10^{-8}$
180	$6.84 \times 10^{-7}$

were dipped again in a KCl solution and produced voltammograms similar to those previously obtained, except at lower intensities. In contrast, when the LB films were removed and again immersed in the test solution, considerable changes occurred and the films could not be reused.

In order to study the reproducibility of the EPD technique, nine identical electrodes were prepared and tested in a 0.1 M KCl solution. The values of the peak potentials were highly reproducible with standard deviations of 2.94%, 8.70%, 4.54%, and 1.64% for peaks I anodic ( $I_a$ ), I cathodic ( $I_c$ ), II anodic ( $II_a$ ), and II cathodic ( $II_c$ ), respectively (Figure 8a). These values were similar to those obtained in the LB films where the standard deviations were 1.14%, 0.89%, 1.58%, and 0.84% for peaks  $I_a$ ,  $I_c$ ,  $II_a$ , and  $II_c$  respectively.

The influence of the nature of the electrolytic solution on the electrochemical response of the EPD  $\text{LuPc}_2$  films was tested by immersing the electrodes in solutions containing KCl,  $\text{MgCl}_2$ ,  $\text{KClO}_4$ , HCl, and NaOH (all the concentrations were 0.1 M). The studies were carried out using the EPD electrodes deposited at 180 s. The results are depicted in Figure 8.

Using  $\text{MgCl}_2$  as an electrolyte (Figure 8b), the voltammograms obtained were similar to those recorded in the KCl solution (Figure 8a). In this case (when  $\text{MgCl}_2$  is used as an electrolyte), the peaks appear at  $E_{1/2} = 0.57$  V for peak I and  $E_{1/2} = -0.34$  V for peak II. The similarities in the responses in KCl and in  $\text{MgCl}_2$  indicate that, during oxidation and reduction, anions (and not cations) are incorporated into the film to compensate the generated positive charges. Similarly, during reduction, anions are expelled from the film to maintain the electroneutrality of the electrode.

In the presence of  $\text{KClO}_4$  (Figure 8c), the oxidizing character of the  $\text{ClO}_4^-$  anion incorporated into the film facilitates the oxidation of the phthalocyanine molecules. The values obtained for peak I and peak II were  $E_{1/2} = 0.44$  V and  $E_{1/2} = -0.45$  V, respectively. In acid media (HCl) (Figure 8d), the response of the electrode differed significantly from those observed in neutral solutions. It is well-known that acidic solutions may protonate the reduced form of  $\text{LuPc}_2$  and then induce a disproportionation reaction causing the production of two oxidation processes: the expected peak at 0.75 V and of a new peak at 0.28 V associated with the oxidation of the protonated form.<sup>41</sup> In basic media (NaOH) (Figure 8e), the redox activity of the bisphthalocyanine

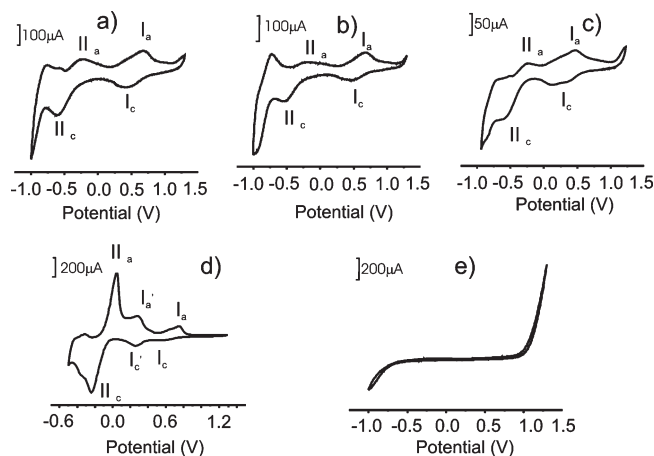


**Figure 8.** CV curves of  $\text{LuPc}_2$  film electrode (180 s) immersed in 0.1 M aqueous solutions: (a) KCl; (b)  $\text{MgCl}_2$ ; (c) HCl; (d)  $\text{KClO}_4$ ; and (e) NaOH.

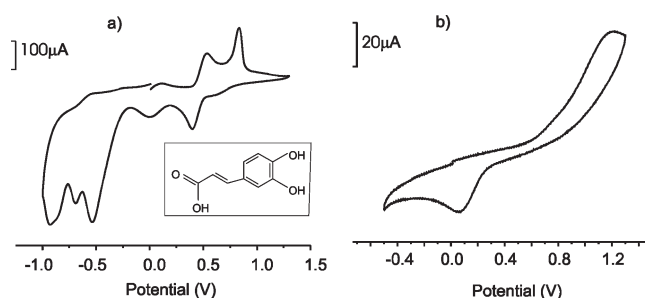


**Figure 9.** Cyclic voltammogram of (a) EPD electrode modified with  $\text{LuPc}_2$  and (b) a bare ITO electrode, immersed in a caffeic acid solution ( $5 \times 10^{-4}$  M). The inset shows the formula of the caffeic acid.

was not observed. This result is in accordance with previously published results, where carbonous electrodes chemically modified with lanthanide bisphthalocyanines have been exposed to biogenic amines.<sup>43</sup> In strongly basic pHs, the oxidation and reduction of the phthalocyanine ring occur at potentials out of the working range.

In summary, depending on the nature of the electrolytic solution, the electrode covered with  $\text{LuPc}_2$  nanowires showed characteristic electrochemical responses. This variety of responses makes these electrodes appropriate to use as a sensing unit of an electronic tongue (an array of sensing units with cross-selectivity, coupled with pattern recognition techniques).<sup>44</sup> In these systems, the electrochemical signals produced by the array immersed in different solutions (training set) are used to train a pattern recognition software. Using predictive chemometric techniques, it is possible to recognize unknown solutions by comparing the responses of the analyte with the signals of the training set.<sup>45</sup>

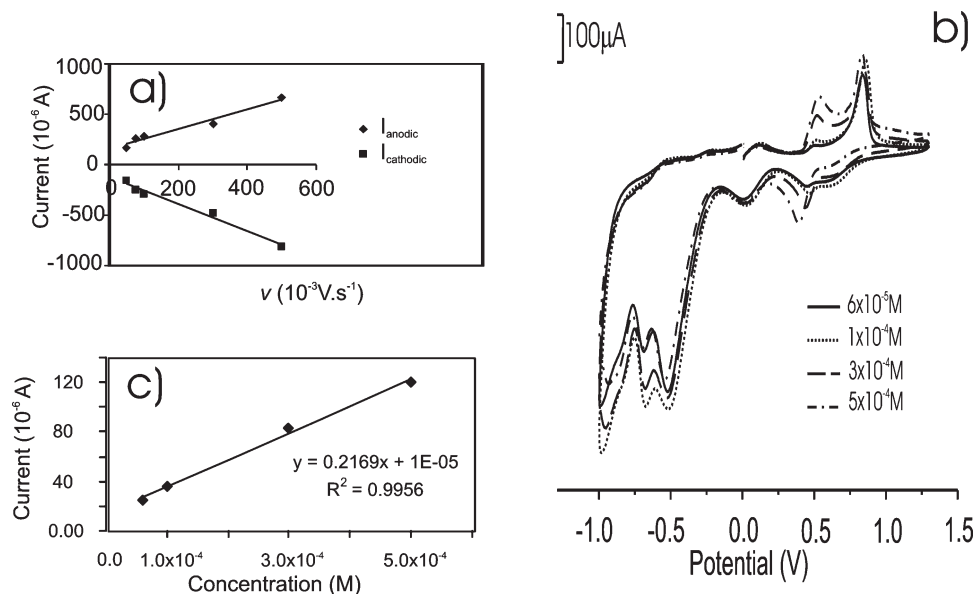
**3.3. Detection of Caffeic Acid.** One of the main challenges in the field of multisensor systems (e-tongues) is the development of new sensors able to detect non-ionic analytes. In order to evaluate the possible application of the  $\text{LuPc}_2$  films as sensor of non-ionic solutions, the electrochemical response toward caffeic acid was tested.

Figure 9 shows the electrochemical response of the EPD-film and a bare ITO film immersed in a solution of  $5 \times 10^{-4}$  M caffeic

(43) Rodríguez-Méndez, M. L.; Apetrei, C.; Gay, M.; De Saja, J. A. *Electrochim. Acta* **2009**, *54*, 7033–7041.

(44) Gutierrez, J. M.; Moreno-Baron, L.; Pividori, M. I.; Alegret, S.; Del Valle, M. *Microchim. Acta* **2010**, *169*, 261–268.

(45) Escuder-Gilabert, L.; Peris, M. *Anal. Chim. Acta* **2010**, *665*, 15–25.



**Figure 10.** (a) Plot of the intensity of the peaks associated with caffeic acid vs the scan rate. (b) Linear relationship of the intensity of the peaks associated to caffeic acid vs the concentration. (c) Cyclic voltammograms of the EPD film immersed in caffeic acid from  $6 \times 10^{-5}$  M to  $5 \times 10^{-4}$  M.

acid (pH = 3.6). The voltammogram obtained (Figure 9a) differs significantly from the voltammograms recorded in the ionic solutions shown in Figure 8. The curve is characterized by (i) a peak at  $E_{1/2} = 0.47$  V associated with the two-electron reversible oxidation of caffeic acid;<sup>46</sup> (ii) the characteristic peaks associated with the oxidation and reduction of the lutetium bisphthalocyanine in acidic media at  $E_{1/2} = -0.11$  V,  $E_{1/2} = 0.27$  V, and  $E_{1/2} = 0.70$  V.

It is important to remark that the interactions between the caffeic acid and the bisphthalocyanine cause changes in the intensities and positions of the peaks expected for both components analyzed separately. For example, the antioxidant character of the caffeic acid shifts the oxidation of the phthalocyanine to higher potentials (from 0.71 V to 0.84 V). In turn, the electrocatalytic effect of the phthalocyanine favors the oxidation of the caffeic acid that shows the anodic peak at 0.54 V instead of at 1.2 V observed when using a bare ITO electrode.

All these effects and interactions responsible for the distinct response of this electrode to caffeic acid. In fact, the response is different from the responses previously published using carbon paste or LB lutetium bisphthalocyanine electrodes immersed in model solutions of basic tastes<sup>14</sup> and bitterness,<sup>47</sup> biogenic amines,<sup>43</sup> other antioxidants,<sup>32</sup> and complex solutions containing a mixture of ions and antioxidants such as wines.<sup>48,49</sup>

Kinetic studies have been carried out (Figure 10a) by recording the cyclic voltammograms of the EPD-LuPc<sub>2</sub> electrode immersed in  $5 \times 10^{-4}$  M caffeic acid at different scan rates (from 0.05 to 0.5 V.s<sup>-1</sup>). The intensity of the redox peaks associated with the caffeic acid (at  $E_{1/2} = 0.47$  V) increased linearly with the scan rate, indicating the dominance of the surface confined processes. The surface coverage ( $\Gamma$ ) can be calculated using the Laviron equation

$$I = nF^2vA\Gamma/4RT \quad (2)$$

(46) Giacomelli, C.; Ckless, K.; Galato, D.; Miranda, F. S.; Spinelli, A. *J. Braz. Chem. Soc.* **2002**, *13*, 332–338.

(47) Apetrei, C.; Rodríguez-Méndez, M. L.; Parra, V.; Gutierrez, F.; de Saja, J. A. *Sens. Actuators, B* **2004**, *103/1–2*, 145–152.

(48) Apetrei, C.; Apetrei, I.; Nevares, I.; del Alamo, M.; Parra, V.; Rodríguez-Méndez, M. L.; De Saja, J. A. *Electrochim. Acta* **2007**, *52*, 2588–2594.

(49) Parra, V.; Arrieta, A.; Fernández-Escudero, J. A.; Rodríguez-Méndez, M. L.; de Saja, J. A. *Sens. Actuators, B* **2006**, *118*, 448–453.

where  $n$  is the number of electrons,  $F$  the Faraday constant,  $v$  the rate,  $A$  the area of the sensor,  $\Gamma$  the surface coverage,  $R$  the gas constant, and  $T$  the temperature. The surface coverage of the EPD-LuPc<sub>2</sub> film calculated using eq 2 for the anodic wave (at 0.54 V) was  $2.45 \times 10^{-10}$  mol.cm<sup>-2</sup>. This value is higher than that obtained using a bare ITO electrode ( $2.37 \times 10^{-11}$  mol.cm<sup>-2</sup>) indicating that, when the nanostructured sensor was employed as the electrode, the oxidation of the caffeic acid was favored.

As shown in Figure 10b,c, the intensity of the peak at 0.54 V was linearly dependent with the concentration of caffeic acid in the range from  $6 \times 10^{-5}$  M to  $5 \times 10^{-4}$  M with a detection limit of  $3.12 \times 10^{-5}$  M.

These results demonstrate that the LuPc<sub>2</sub> film provides a distinct and reproducible response to caffeic acid, and that the sensor can be used to quantify the presence of the antioxidant in the range usually present in foods.

#### 4. Conclusions

LuPc<sub>2</sub> nanowires have been successfully deposited onto ITO substrates by the EPD technique. The structure of the nanowires has been analyzed by means of spectroscopic and microscopic techniques confirming the stacking of the molecules perpendicular to the substrate and the coexistence of a herringbone structure. The size of the nanowires and the roughness of the films can be controlled by the deposition time.

Highly stable and reproducible cyclic voltammograms can be obtained by annealing the films, because the thermal process increases the adhesion of the films to the substrate. The electrochemical behavior is similar to that previously observed in LB films with some differences in the position, intensity, and shape of the peaks. Such differences are associated with the different organization of the molecules in EPD films. The electrochemical responses depend on the nature of the electrolytic solution. As expected for diffusion-controlled processes, the intensities of the peaks are linearly dependent with the square root of the scan rate.

The electrodes have been successfully used as sensors for the detection of caffeic acid. The interactions between the antioxidant and the electrochemical material are responsible of the specific response for the electrodes to caffeic acid and the voltammograms can be considered as a fingerprint of this compound. A detection limit of

$3.12 \times 10^{-5}$  M has been attained, which is in the range of the concentration of caffeic acid found in several foods.

In comparison with LuPc<sub>2</sub> LB films, the EPD LuPc<sub>2</sub> films allow the development of nanostructured sensors at lower costs and in a shorter time. Also, the EPD technique is reliably reproducible.

**Acknowledgment.** Financial support by the Spanish Ministry of Science (grant AGL2009-12660/ALI) is gratefully acknowledged.

MGM also thanks the Spanish Ministry of Education for a fellowship (F.P.I, AGL2006-05501). Central de Tecnología del Instituto de Sistemas Optoelectrónicos y Microtecnología (CT-ISOM) is also gratefully acknowledged.

**Supporting Information Available:** Additional figures as described in the text. This material is available free of charge via the Internet at <http://pubs.acs.org>.